Polymeric Nanoarchitectures: Advanced Cargo Systems for Biological Applications

Yingtong Luo, Yudong Li, Loai K. E. A. Abdelmohsen, Jingxin Shao,* and Jan C. M. van Hest*

Polymeric nanoarchitectures are crafted from amphiphilic block copolymers through a meticulous self-assembly process. The composition of these block copolymers is finely adjustable, bestowing precise control over the characteristics and properties of the resultant polymeric assemblies. These nanoparticles have garnered significant attention, particularly in the realm of biological sciences, owing to their biocompatibility, favorable pharmacokinetics, and facile chemically modifiable nature. Among the myriad of polymeric nanoarchitectures, micelles and polymersomes stand out as frontrunners, exhibiting much potential as cargo carrier systems for diverse bio-applications. This review elucidates the design strategies employed for amphiphilic block copolymers and their resultant assemblies, specifically focusing on micelles and polymersomes. Subsequently, it discusses their wide-ranging bio-applications, spanning from drug delivery and diagnostics to bioimaging and artificial cell applications. Finally, a reflective analysis will be provided, highlighting the current landscape of polymeric cargo carriers, and discussing the opportunities and challenges that lie ahead. With this review, it is aimed to summarize the recent advances in polymeric assemblies and their applications in the biomedical field.

1. Introduction

Polymeric nanoarchitectures comprised of amphiphilic block copolymers have emerged as versatile and efficient platforms in the realm of biological applications. This is attributed to their inherent ability to be easily tailored to specific requirements, especially when compared to their lipid counterparts.[1–5] By finely adjusting the hydrophilic/hydrophobic ratio, these synthetic building blocks can spontaneously assemble into a myriad of nanostructures, including micelles, vesicles, and fibers.[6–9]

Y. Luo, Y. Li, L. K. E. A. Abdelmohsen, J. Shao, J. C. M. van Hest
Bio-Organic Chemistry
Institute for Complex Molecular Systems
Eindhoven University of Technology
Eindhoven 5600 MB, The Netherlands
E-mail: j.shao@tue.nl; J.C.M.v.Hest@tue.nl

The ORCID identification number(s) for the author(s) of this article can be found under https://doi.org/10.1002/mabi.202400540

Furthermore, the organization of these building blocks into nanoparticles can be modulated by self-assembly processes such as solvent switch, film rehydration, and double emulsion methods.[10–12] Given the in vivo delivery challenges associated with molecular therapeutics like drugs, nucleic acids, and imaging agents, there is a clear necessity for protective cargo carriers. Micelles and polymersomes, serving as classical cargo-carrying systems, have demonstrated exemplary capability in terms of cargo loading (**Figure 1**).[13,14] Functional molecules can be introduced during the self-assembly process, facilitating their encapsulation by non-covalent interactions.[15] Apart from this physical encapsulation, functional molecules can also be incorporated into the block copolymer via chemical modification. Various functional groups such as targeting ligands, imaging agents, drug payloads, or stimuli-responsive moieties can as such be incorporated into the assemblies.[16–20] Furthermore, post-assembly modifications, such as click chemistry and chemical/physical metal deposition, have proven to be efficient approaches for functionalizing polymeric nanoparticles.[21,22] Over the past few decades, with advancements in polymer chemistry and nanotechnology, polymer assemblies have significantly expanded their potential, catering to diverse requirements across various biomedical applications.[23–25]
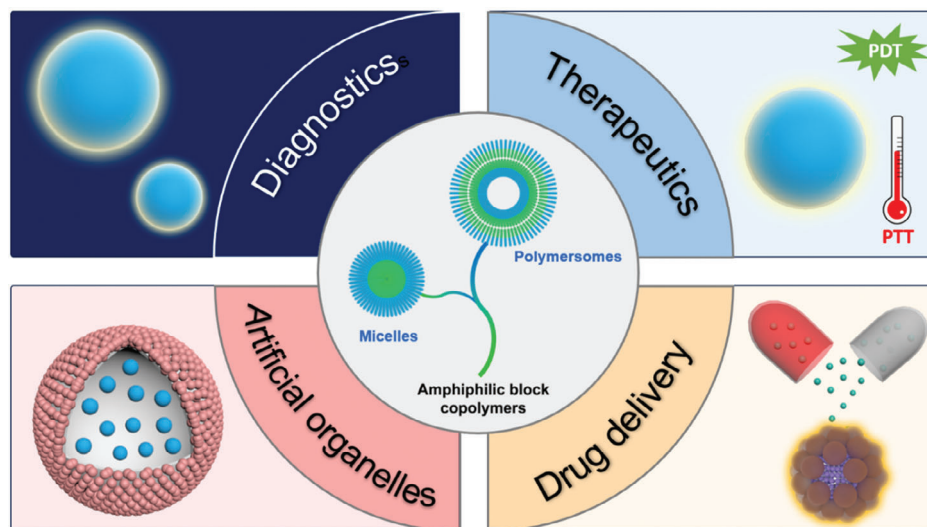
In this review, we describe the relationship between polymer structure, assembly process, and biomedical applications. Beginning with the fundamental design, we explore the synthesis methods of amphiphilic block copolymers and discuss the key principles underlying the synthesis procedures. Furthermore, we provide an overview regarding self-assembly processes in relation to the physicochemical properties of these block copolymers, such as the hydrophilic/hydrophobic balance and molecular weight, and how they influence the formation, stability, and morphology of the resulting polymeric nanoarchitectures. Finally, the structural features and functionalities of the nanostructures, along with their suitability for various biomedical applications, such as therapeutics, diagnostics, drug delivery, and artificial organelles will be discussed. Through this review, we hope to provide more insight into polymer nanoarchitectures, from their synthesis to their potential applications, to guide future research and applications in the biological field.

**ADVANCED
SCIENCE NEWS**

www.advancedsciencenews.com

Macro-
olecular
Bioscience

www.mbs-journal.de

Figure 1. Overview of micelles and polymersomes as cargo carriers for biomedical applications.

2. Synthesis of Amphiphilic Block Copolymers

Advancements in polymer chemistry over the past decades have made it possible to synthesize a range of novel block copolymers with different structural compositions to address the specific demands of various biomedical applications.[26,27] Controlled polymerization techniques, regarded as the most versatile and facile approaches, are extensively employed in polymer synthesis. These techniques encompass atom transfer radical polymerization (ATRP), reversible addition–fragmentation chain transfer (RAFT) radical polymerization, and ring-opening polymerization (ROP). They enable the synthesis of polymers with well-defined structures, controlled molecular weight distributions, and functional end-groups.[28–31] ATRP and RAFT, initially reported in 1995 and 1998, respectively, have emerged as the two most common controlled radical polymerization methods.[29,32] Notably, these methods allow for polymerization in aqueous solvents, a feat that cannot be simply achieved through ROP.[33,34]
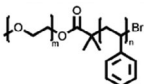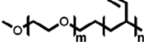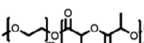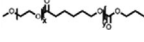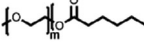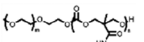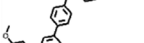
A summary of common amphiphilic block copolymers and their synthetic methods is provided in **Table 1**. End-group functionalized PEG is most often utilized as a macroinitiator for copolymer synthesis, as it will form the hydrophilic outer shell of the particles after polymer assembly where it prolongs blood circulation time in vivo, which enhances drug accumulation and reduces side effects.[35] Copolymers such as PEG-b-PS and PEG-PBD are typically obtained through free radical polymerization, as their monomers contain the necessary vinyl units. Conversely, for biodegradable block copolymers like PEG-PCL, PEG-PLA, PEG-PTMC, and their derivatives, ROP is applied for synthesis. Additionally, the synthesis of functionalized block copolymers can be achieved through a combination of traditional polymerization methods and chemical modifications.[36,37]

3. Amphiphilic Block Copolymers for Self-Assembly

The size and morphology of polymeric nanoassemblies play a crucial role in determining their effectiveness in biological applications. These factors significantly impact essential processes such as biodistribution, tissue penetration, endocytosis efficiency, and drug release capability for drug delivery systems.[38] Therefore, it is imperative to prepare nanoparticles that fulfill various requirements by employing suitable molecular design strategies and assembly techniques. In light of this necessity, we have compiled different parameters influencing nanoparticle formation. During the self-assembly process, the hydrophilic segments extend toward the aqueous phase, forming an external corona, while the hydrophobic segments stack together to create a hydrophobic core. This ordered arrangement not only influences the overall size and morphology of the nanoparticles but also governs their behavior and functionality in biological environments. By understanding and controlling these fundamental aspects of nanoparticle assembly, researchers can tailor their properties to meet specific application needs. The primary driving force behind assembly stems from the interaction between the hydrophobic blocks of the amphiphilic block copolymers. The relative mass or volume fraction plays a crucial role in determining the final morphology, ranging from micelles to polymersomes (**Figure 2**).[39] Specifically, the volume fraction (f), defined as the ratio of the hydrodynamic volume of the hydrophilic block to the total polymer volume, is a good indication of the ultimate assembly morphology.[2] Different morphologies correspond to distinct ranges of f. For instance, when $0.25 < f < 0.4$, vesicles are prone to form; for $0.4 < f < 0.5$, the formation of rodlike micelles is favored; and when f exceeds 0.5, spherical micelles prevail.[40–42] In addition to molecular composition, achieving thermodynamic equilibrium is crucial in the assembly process.[43,44] As self-assembly progresses, the reduction in interfacial energy at the hydrophobic-hydrophilic interface, along with the ordered stacking of unimers, collectively drive the reduction of the system's free energy. This leads to the system reaching an equilibrium state with minimal free energy, facilitating the formation of stable nanostructures. Based on this principle, several factors influence the formation of polymeric nanoparticles, including the self-assembly method, the polymer concentration, and water content.[45] After synthesizing the block

ADVANCED
SCIENCE NEWS
www.advancedsciencenews.com

Macro-
molecular
Bioscience
www.mbs-journal.de

Table 1. Examples of amphiphilic block copolymers discussed in this review, including their synthetic routes, methods of assembly, and applications.
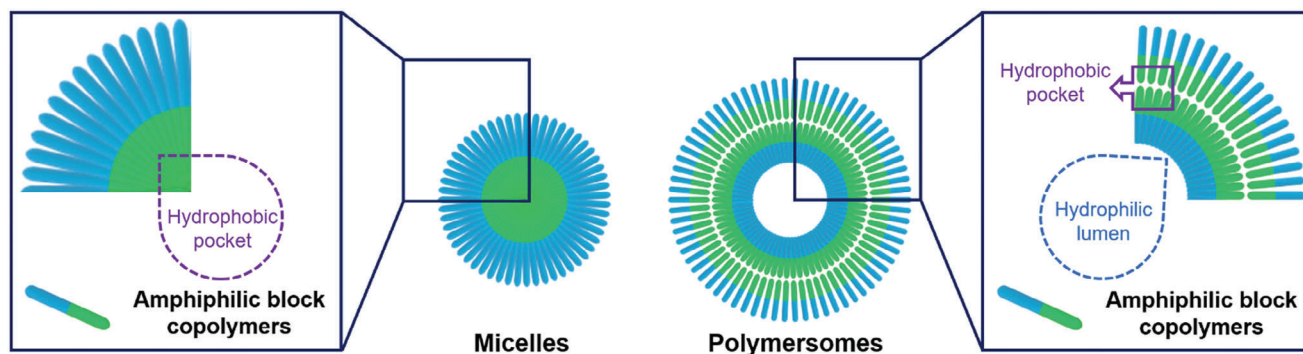
Polymer Structure	Synthetic method	Assembly methods	Resulting nanostructures	Application	Reference
 PEG$_m$-b-PS$_n$	ATRP	Solvent switch	Stomatocytes	Nanomotor	[96]
 PEG$_m$-PBD$_n$	ATRP	Film rehydration	Polymersomes	Magnetic resonance imaging	[79]
 PEG$_m$-PDLLA$_n$	ROP	Solvent switch	Polymersomes	Nanomotor	[78]
 PEG$_x$-PCL$_y$-PTMC$_z$	ROP	Film rehydration	Micelles	Drug delivery	[56]
 PEG$_m$-PCL$_n$	ROP	Single emulsion method	Micelles	Drug delivery	[57]
 PEG$_m$-AIE$_n$	ROP + post-polymerization modification	Solvent switch	Polymersomes	Photodynamic therapy	[80]
 PEG$_m$-PTA$_n$	ROP + post-polymerization modification	Solvent switch	Polymersomes	Photothermal therapy	[81]
 PEG$_x$-P(S$_y$-co-TMI$_z$)	RAFT	Solvent switch	Polymersomes	Enzyme Catalysis	[82]

PEG-b-PS: poly(ethylene glycol)-b-poly(styrene), PEG-PBD: poly(ethylene glycol)-b-poly(butadiene), PEG-PDLLA: poly(ethylene glycol)-b-poly(D,L-lactide), PEG-PCL-PTMC: poly (ethylene glycol)-poly(ϵ-caprolactone)-poly(trimethylene carbonate), PEG-PCL: poly(ethylene glycol)-b-poly(ϵ-caprolactone), PEG-PTMC: poly(ethylene glycol)-b-poly(trimethylene carbonate), PEG-AIE: PEG-PTMC, of which the TMC part is modified with aggregation-induced emission (AIE) photosensitizers, PEG-PTA: PEG-PTMC, of which the TMC part is modified with photothermal agents, PEG-P(Sy-co-TMIz): poly(ethylene glycol)-b-poly (styrene-co-3-isopropenyl-a,a-dimethylbenzylisocyanate).

copolymer, selecting appropriate assembly methods is crucial for forming well-defined polymeric nanoparticles. These assembly techniques can be classified into two categories: solvent-free methods and solvent displacement methods, based on whether organic solvents are used in the self-assembly process.[3] Solvent-free methods include film rehydration and polymerization-induced self-assembly (PISA), where the amphiphilic block copolymers are directly assembled into nanoparticles in an aqueous solution. In contrast, organic solvents are essential in the solvent displacement methods for nanoparticle formation. This section will discuss the main assembly methods.

3.1. Film Rehydration

Film rehydration is the most common technique for the preparation of vesicles due to its simplicity.[46] Initially, amphiphilic block copolymers are dissolved in an organic solvent and deposited on a solid surface. As the solvent evaporates, a film is formed. When an aqueous solution is added, the film swells, and the vesicles detach from the surface. While film rehydration is a straightforward method for vesicle preparation, it results in a fairly broad size distribution of vesicles. To narrow the size distribution, vesicles can be extruded through a filter with specific pore diameters.[47]

**ADVANCED
SCIENCE NEWS**

www.advancedsciencenews.com

[M] acro-
molecular
Bioscience
www.mbs-journal.de

Figure 2. Schematic representing the construction of micelles and polymersomes from amphiphilic block copolymers.
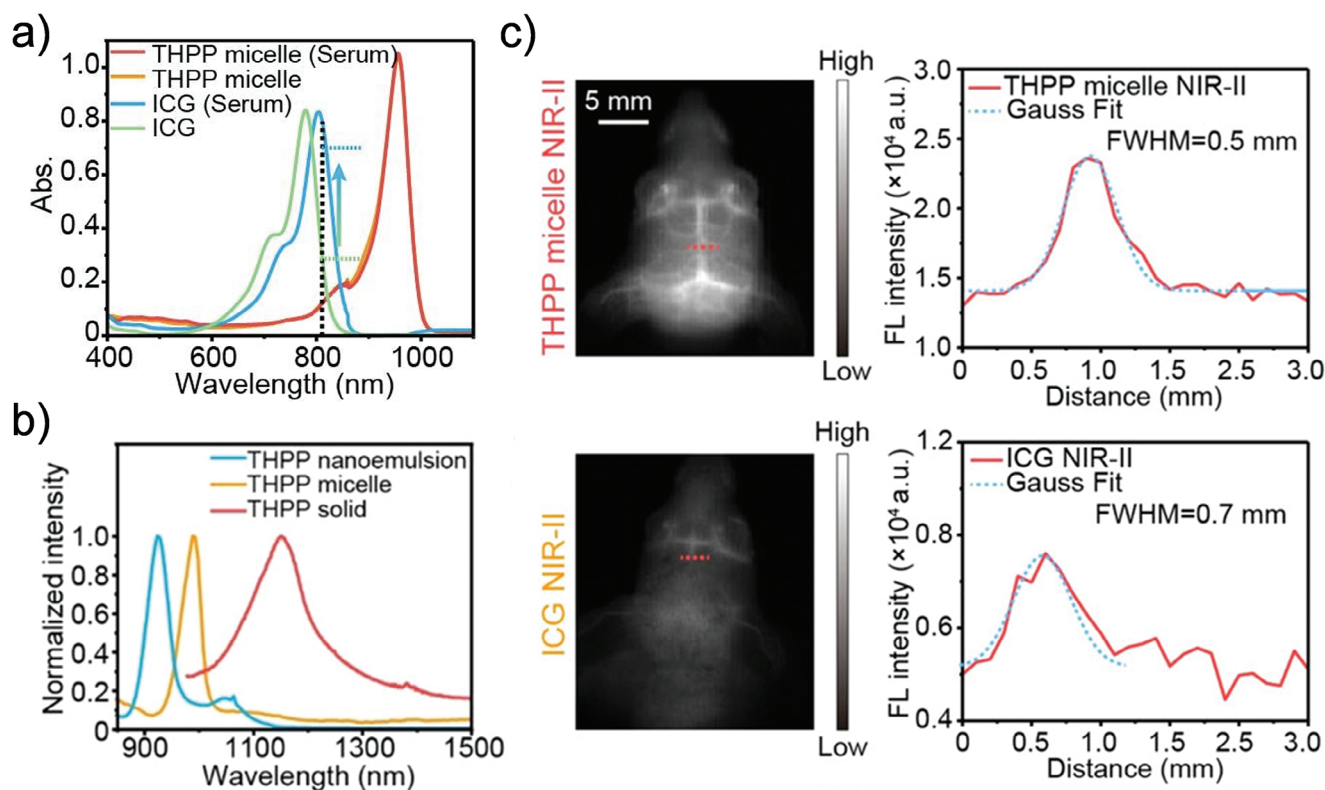
Figure 3. Fluorescent micelles for NIR-II imaging. a) Absorption spectra of THPP micelles, THPP micelles (Serum), ICG and ICG (Serum). b) Normalized emission spectra of micelles, nanoemulsions, and THPP aggregates. c) Cerebral vasculature imaging and fluorescence intensity profiles from the dashed red line of THPP micelles (above), and ICG (below) in the NIR-II window. Reproduced with permission.[61] copyright 2020 John Wiley and Sons.

3.2. Polymerization-Induced Self-Assembly

Polymerization-induced self-assembly (PISA) is an extremely versatile method for the in situ preparation of nanoparticles by combining polymerization and self-assembly.[48] This method leverages the difference in solubility between polymers and monomers in solution. As the polymerization reaction progresses, hydrophobic monomers are polymerized from a hydrophilic macroinitiator, increasing the hydrophobicity of the block copolymer. Once a critical hydrophobic chain length is reached, the self-assembly process occurs, forming polymer particles. The final morphology of the self-assembled nanostructures can be controlled by regulating the degree of polymerization during PISA.[49]

3.3. Solvent Switch Method

In the solvent-switch method, block copolymers are dissolved in an organic solvent that is fully miscible with water. Water is then slowly added to the polymer solution via a syringe pump. The block copolymer becomes more insoluble due to the increased interfacial tension between the hydrophobic block and

2400540 (4 of 16)

ADVANCED
SCIENCE NEWS
www.advancedsciencenews.com

[M] acro-molecular
Bioscience
www.mbs-journal.de
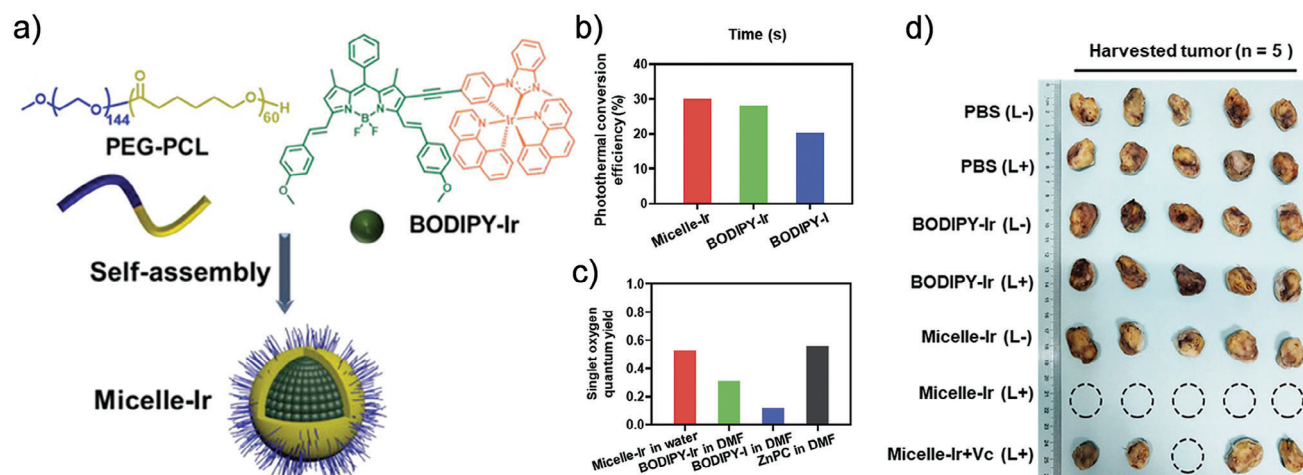
Figure 4. PEG-PCL functional micelles (Micelle-Ir) for in vivo synergistic photodynamic and photothermal treatment. a) Schematic representations of encapsulation of BODIPY-Ir into micelles for constructing Micelle-Ir. b) Photothermal conversion efficiency of Micelle-Ir, BODIPY-Ir, and BODIPY-I. c) $^1O_2$ quantum yield of Micelle-Ir, BODIPY-Ir, and BODIPY-I using DPBF as a probe. d) Pictures of the orthotopic 4T1-Luc tumors harvested from the sacrificed mice at the end of the treatment experiments (Vc: ROS scavenger vitamin C). Reproduced with permission.[62] copyright 2021 John Wiley and Sons.

the surrounding water molecules, consequently triggering self-assembly. Finally, the organic phase is removed through dialysis against an aqueous medium. This method allows for the formation of nanoparticles with a relatively narrow size distribution compared to the film rehydration method. However, it is challenging to avoid residual organic solvents, which can be harmful in biomedical applications.[24]

3.4. Microfluidics for Vesicle Formation

Compared to common solvent displacement methods, microfluidic techniques provide more precise control over the self-assembly process.[50] Microfluidic techniques involve two steps: i) an aqueous core is stabilized by an oil shell containing block copolymers to produce core-shell emulsion droplets using a microfluidic system. ii) These droplets are injected through a second junction into an amphiphile-containing aqueous phase, resulting in the formation of vesicles. By designing the microfluidic device, the size and shape of the resulting particles can be precisely controlled.

4. Micelles and Their Applications

Micelles are core/shell structural nanoparticles that are formed when the concentration of the building blocks exceeds the critical micelle concentration.[51–53] The hydrophobic tails align within the core, while the hydrophilic heads extend outward. Thanks to their sizable hydrophobic core, micelles have a higher loading capacity for hydrophobic cargo compared to their vesicle counterparts.[54] Simultaneously, the outer shell composed of hydrophilic segments acts as a barrier, shielding the cargo from the surrounding environment, thus enhancing cargo stability and reducing systemic toxicity. Because of these features, micelles
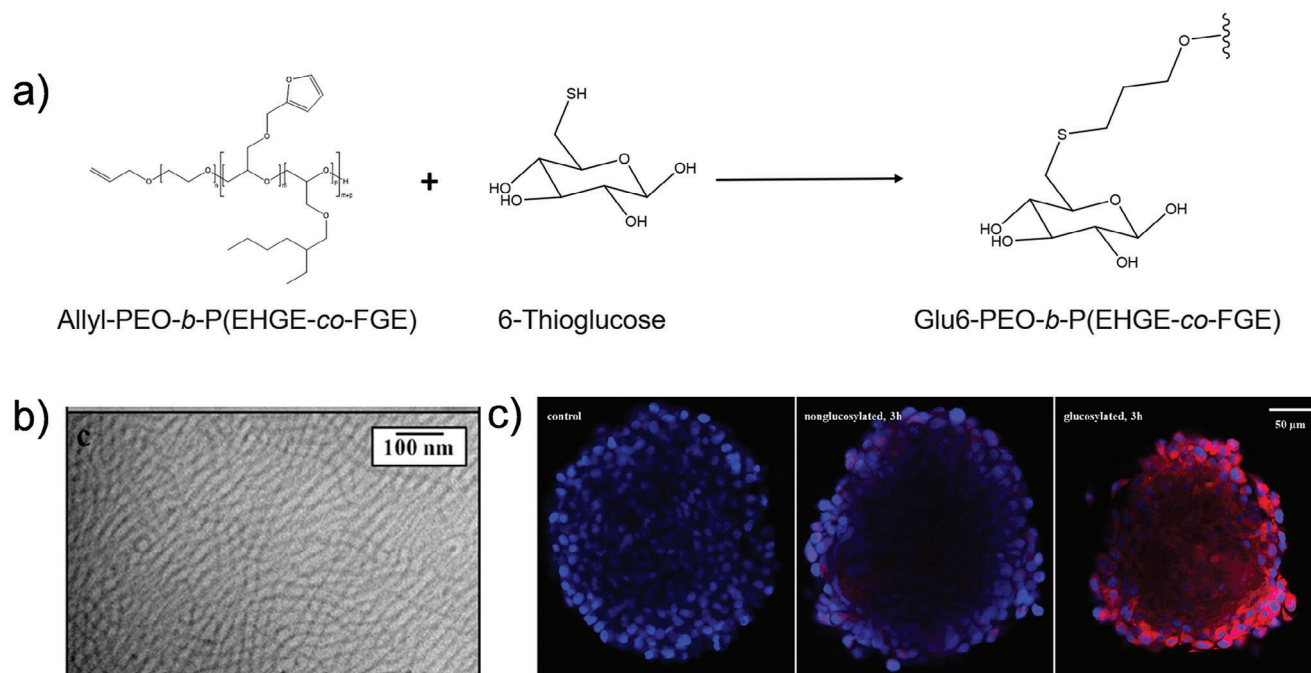
have been extensively explored as drug carrier platforms.[55] For example, Yang et al. utilized a biodegradable block copolymer (PEG-PCL-PTMC) to fabricate curcumin-loaded micelles using a film rehydration method. Subsequent in vitro anticancer studies confirmed significant enhancements in curcumin cellular uptake and apoptosis induction when the micellar system was compared to free hydrophobic curcumin.[56] In another study, Zhang and co-workers prepared gambogic acid-loaded micelles (GA-micelles) employing a modified single emulsion method. Both in vitro and in vivo investigations demonstrated the effectiveness of PEG-PCL micelles as a drug delivery system in enhancing the anticancer efficacy of GA against gastric cancer. The notable therapeutic effect of GA-micelles in vivo was attributed to various factors, including sustained drug release, enhanced cellular uptake, and improved stability and aqueous solubility of GA encapsulated within the nanoparticles.[57] Yang et al. prepared arenobufagin-loaded micelles from PEG-PLA using a thin film hydration method, resulting in micelles exhibiting high drug loading content (7.3–7.5%) and encapsulation efficiency (80.3–82.5%). In vivo, anticancer experiments confirmed that the tumor-inhibition rate of these drug-loaded micelles (72.9%) was 1.28-fold higher than that of free arenobufagin (57.1%). Furthermore, these micelles effectively limited the leakage of arenobufagin, thus reducing side effects on normal tissue.[58] PEG-PDLLA micelles are also widely used in drug delivery due to their excellent biocompatibility and degradability. Guan et al. developed pH-responsive micelles modified with the binding peptide PSBP-6 to enhance antitumor drug delivery. They first synthesized poly(ethylene glycol)-b-poly(L-histidine) (PEG-PHIS), featuring a pH-responsive block (PHIS), and a copolymer modified with the phosphatidylserine-binding peptide (PSBP-6-PEG-PDLLA) as a targeting component. The resulting multifunctional micelles demonstrated significant potential for targeted drug delivery, offering promising prospects for improved tumor treatment.[59] Furthermore, micelles possessed the ability to overcome the
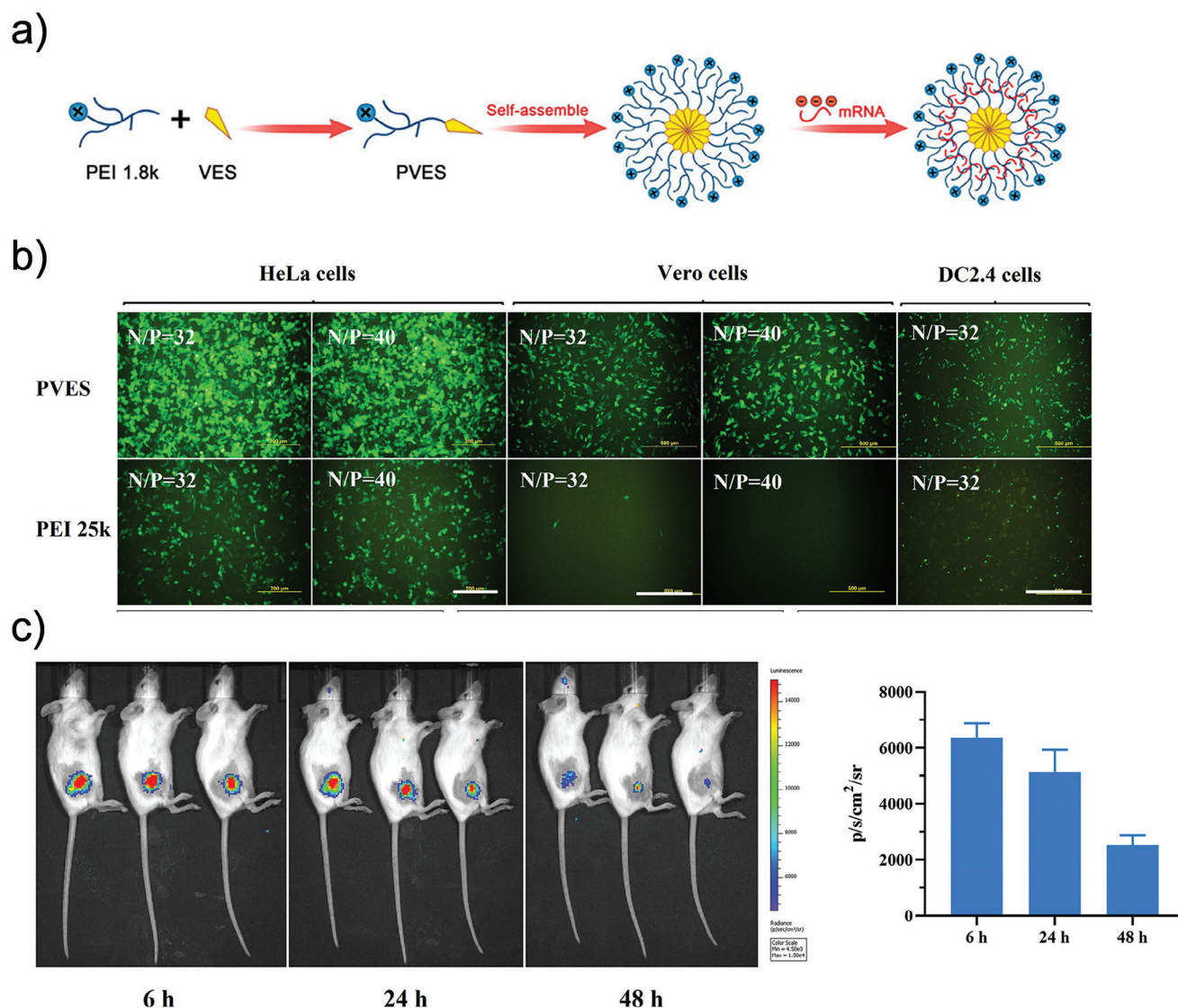
Figure 5. Micelles based on polyethyleneimine (PEI) modified with vitamin E succinate (PVES) for mRNA vaccine delivery. a) Schematic illustrating the synthesis of PVES and PVES/mRNA vaccine. b) PVES/mRNA transfection efficiencies in HeLa and Vero cells at N/P ratios of 32 and 40; PVES/mRNA transfection efficiency in DC2.4 cells at N/P ratios of 32. Scale bar 200 µm in HeLa cells and 500 µm in Vero and DC2.4 cells. c) Bioluminescent images to detect luciferase expression in mice 6 h, 24, and 48 h after i.m. injection of PVES/luciferase mRNA (left). Quantified fluorescence signals in regions of interest (ROIs) (right). Reproduced with permission.[63] copyright 2021 Elsevier Science B.V.

challenges of immunotherapy. Sun et al. prepared maleimide-modified resiquimod (R848) nanoparticles (MAL-NPs) using MAL-PEG-PDLLA copolymers. When combined with radiotherapy (RT), MAL-NPs significantly enhanced antigen uptake by dendritic cells and improved nanoparticle accumulation at tumor sites. Moreover, MAL-NPs underwent selective radio-reduction upon RT stimulation, leading to the release of R848 in vivo. After 24 hours, the concentration of R848 within the tumor was 11.20-fold higher than that in the liver, significantly enhancing the antitumor effect.[60] Organic small molecule photosensitizers can also be effectively encapsulated by amphiphilic block polymers through hydrophobic interactions to prepare contrast or therapeutic agents. For example, Zhang et al. prepared a NIR-II fluorescent contrast agent through encapsulation of a small molecule dye (THPP) into PEO-PPO-PEO micelles. By manipulating the molecular aggregation state (from H-aggregates to J-aggregates), the fluorescence intensity of the dye was substantially enhanced (≈55-fold), and the maximal absorption/emission wavelengths were attained in the NIR-II region (**Figure 3**a,b). Furthermore, THPP micelles and their protein complex (THPP micelle (Serum)) showed an intensity enhancement of over 8 times (>1200 nm) compared to the regularly used free ICG and the ICG protein complex (ICG (Serum)) (Figure 3a). THPP micelles were highly suitable for fast NIR-II fluorescent imaging with a valid penetration depth of up to 6 mm, displaying three times higher fluorescence brightness compared to indocyanine green in mice vasculature (Figure 3c). For the application, they succeeded in monitoring the respiratory rate of acute-lung-injury mice and

ADVANCED
SCIENCE NEWS

www.advancedsciencenews.com

[M] acro-
molecular
Bioscience

www.mbs-journal.de

Figure 6. Worm-like micelles for glucose-mediated cargo transport. a) Synthesis of glucose-functionalized polymer (Glu6-PEO-*b*-P(EHGE-*co*-FGE)) b) Cryo-TEM micrographs of core-crosslinked, fluorescent worm-like micelles. c) CLSM images of U87MG spheroids incubated with either 100% glucosylated or 100% nonglucosylated micelles for 3 h at 80 µm depth. Cell nuclei in the incubated samples as well as in the control sample were stained with DAPI (blue). Reproduced with permission.[65] copyright 2021 American Chemical Society.

tracing the collateral circulation process by using those fluorescent micelles.[61]

Micelles can also serve as antitumor agents. Liu et al. developed a neutral Ir(III) complex bearing the distyryl boron dipyrromethene (BODIPY-Ir) photosensitizer. To improve the biocompatibility of the photosensitizer, it was encapsulated into PEG-PCL functional micelles (Micelle-Ir) for in vivo synergistic photodynamic and photothermal treatment, PDT and PTT, respectively (**Figure 4a–c**). 4T1-Luc tumors were effectively killed after this synergistic phototherapy and metastasis to the lungs was prevented through inhibition of the metastasis-relevant proteins and immune response (Figure 4d).[62]

In addition to small molecular drugs, micelles can also serve as a delivery system for nucleic acids such as mRNA. Ren, et al. developed a type of polymeric micelles based on polyethyleneimine (PEI) modified with vitamin E succinate (PVES) for mRNA vaccine delivery. mRNA was encapsulated in micelles through electrostatic interactions (**Figure 5a**). The transfection efficiency of PVES/mRNA complexes was approximately three times higher than the control group of PEI 25K per mRNA complexes in HeLa cells (Figure 5b). Both in vitro and in vivo experiments demonstrated the potential of PVES as a safe and effective delivery carrier for mRNA (Figure 5c).[63]
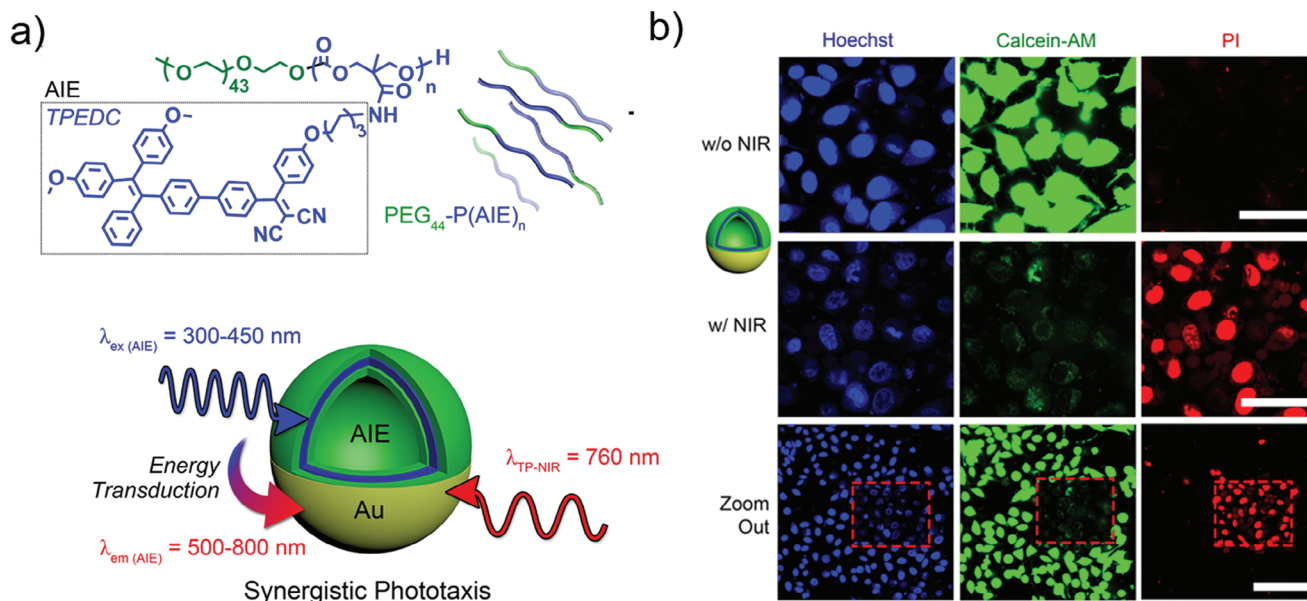
Beyond spherical micelles, non-spherical micelles have also been employed for drug delivery. Notably, non-spherical morphologies often result in higher drug-loading capacities and longer blood circulation times compared to their spherical counterparts.[64] Elter et al. developed core-crosslinked fluorescent worm-like micelles as glucose-mediated drug delivery vehicles. These long worm-like micelles were prepared from gly-

cosylated terpolymers (**Figure 6a**). Despite exhibiting a relatively high contour length of 790 ± 390 nm, the nanocarriers demonstrated effective glucose-mediated transport into appropriate cell lines (Figure 6b,c).[65] Gao et al. designed a rod-like micelle with a diameter of 20 nm and a length of 600 nm, demonstrating a half-life of 24 hours in the bloodstream and enhanced cellular uptake. When loaded with the anticancer drug doxorubicin and magnetic nanoparticles (Fe_3O_4), the rod-like micelles exhibited a strong in vivo antitumor effect, showing an 83% inhibition rate in an H22 hepatocarcinoma tumor model.[66] These examples highlight that polymeric micelles not only enhance the therapeutic effects of loaded drugs but also improve their stability in vivo, emphasizing their potential for anticancer therapy and clinical translation.

5. Polymersomes and their Applications

Polymer vesicles were first described in 1995 by the research groups of Meijer and Eisenberg.[67,68] In 1999, Discher et al. introduced the term "polymersomes" to describe vesicles formed from poly(ethylene oxide)-polyethylene.[69,70] Traditional polymersomes typically exhibit spherical structures with an aqueous compartment in the lumen, encased by a hydrophobic membrane that separates and protects the fluidic core from the external environment. This aqueous lumen is often used to encapsulate hydrophilic biomacromolecules such as proteins (e.g., BSA, antibodies) and nucleic acids (e.g., pDNA and siRNA).[71–74] Additionally, the bilayer can encapsulate hydrophobic molecules. The capability to load multifunctional cargos – particularly those with diverse hydrophobic properties – into polymersomes

**ADVANCED
SCIENCE NEWS**

www.advancedsciencenews.com

**Macro-
molecular
Bioscience**

www.mbs-journal.de

Figure 7. AIE polymersomes with a gold shell for enhanced phototherapy. a) AIE block copolymer (above) and hybrid nanomotor composed of plasmonic Au shell and AIE polymersomes. b) Confocal images showing highly selective cell apoptosis using nanomotors with or without NIR irradiation (nucleus: Hoechst, blue/viable cells: calcein-AM, green/apoptotic cells: PI, red). All scale bars = 50 μm. Reproduced under terms of the CC-BY-NC license.[80]

has been employed for various applications across medicine, pharmacy, and other life sciences fields.[75]
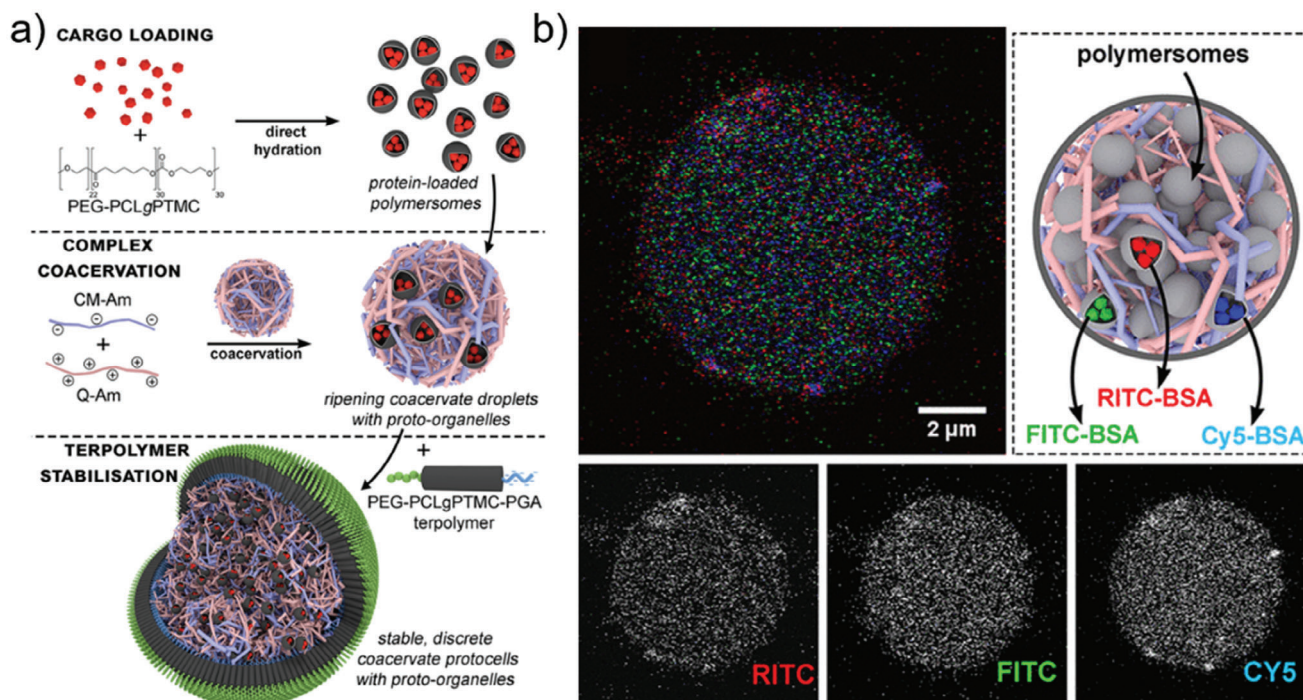
5.1. Spherical Polymersomes

Traditional spherical polymersomes are widely used in drug delivery and controlled release research due to their versatile structural properties, biocompatibility, and ability to encapsulate both hydrophilic and hydrophobic molecules. These vesicular structures protect sensitive therapeutic agents from degradation, improve their stability in biological environments, and facilitate targeted delivery to specific tissues or cells.[39] For example, Wauters et al. loaded β-glucan into the aqueous core of polymersomes, studying their efficacy both as a monotherapy and in combination with anti-PD-1 checkpoint inhibition in the B16F10 mouse melanoma model.[76] They could demonstrate that size played an important effect in polymersome biodistribution, which enabled them to specifically target the spleen as organ of interest to modulate the immune cell response. Zhu and colleagues encapsulated the hydrophobic drug paclitaxel within the thick lamellar membrane and the hydrophilic drug doxorubicin into the aqueous core of polymersomes, enhancing the combination chemotherapeutic effect for cancer cells.[77] Additionally, polymersomes with Janus morphology have been employed in drug delivery as self-propelled systems. For example, Shao et al. engineered light-driven nanomotors utilizing pH-responsive polymersomes coated with a hemispherical gold layer. The Janus morphology enabled these hybrid polymersomes to exhibit photothermal motility by generating thermal gradients under NIR irradiation. Additionally, the pH-sensitive unit allowed for the controlled release of the profluorescent enzyme substrate, facilitating enzymatic catalysis within living cells. These nanomo-

tors have the potential to deliver drug molecules across cellular membranes and achieve controlled cargo release in specific tissues.[78] Yan and colleagues co-assembled PEG-PBD and PEG-PPO-PEG to fabricate porous polymersomes. These doped polymersomes demonstrated enhanced membrane permeability to molecules smaller than 5 kDa, while effectively retaining molecules ≥10 kDa within their aqueous interiors without significant leakage. These bicomponent polymersomes exhibited faster water exchange through the porous membrane compared to non-doped polymersomes, resulting in improved performance in magnetic resonance imaging.[79] Cao et al. synthesized a functional block copolymer through ROP and post-polymerization functionalization which was composed of the block copolymer poly(ethylene glycol)-poly(trimethylene carbonate), in which aggregation-induced emission (AIE) photosensitizers were introduced in the hydrophobic domain as side chains (**Figure 7**a). Following a self-assembly process and subsequent gold coating, the authors generated AIE polymersomes with an asymmetric Au shell. These hybrid particles were capable of harnessing energy from a two-photon near-infrared laser for generation of fluorescence and reactive oxygen species (ROS), which is advantageous for enhanced phototherapy (Figure 7b).[80] Furthermore, the Au layer also resulted in plasmonic heating upon irradiation, leading to a temperature gradient that propelled the particles.

Inspired by Cao's work, Luo et al. designed and synthesized photothermal-responsive polymersomes by incorporating photothermal molecules into an amphiphilic block copolymer. These photothermal vesicles can serve as cargo carriers for both hydrophobic and hydrophilic cargos (e.g., cyanine dye) and also act as agents for photothermal therapy.[81] Lomas et al. designed and synthesized pH-sensitive poly(2-(methacryloyloxy)ethyl-phosphorylcholine)-co-poly(2-(diisopropylamino) ethyl methacrylate (PMPC-PDPA) diblock

**ADVANCED
SCIENCE NEWS**

www.advancedsciencenews.com

[M] acro-
molecular
Bioscience

www.mbs-journal.de

Figure 8. Polymersomes as proto-organelles to mimic cellular compartmentalization. a) Schematic illustrating the formation of a hierarchical artificial cell. b) Artificial cells capable of sequestering three distinct subpopulations of polymersomal proto-organelles, each loaded with fluorescently labeled proteins for targeted compartmentalization and functional differentiation. Reproduced under terms of the CC-BY-NC license.[87]

copolymers and prepared pH-sensitive polymersomes. During assembly, nucleic acids were encapsulated in the lumen. The PDPA block acted as a pH-sensitive unit that became protonated under acidic conditions, transitioning from a hydrophobic to a hydrophilic state. Unlike cationic liposome transfection agents and calcium phosphate particles, PMPC-PDPA polymersomes protect nucleic acids from enzymatic degradation.[82]
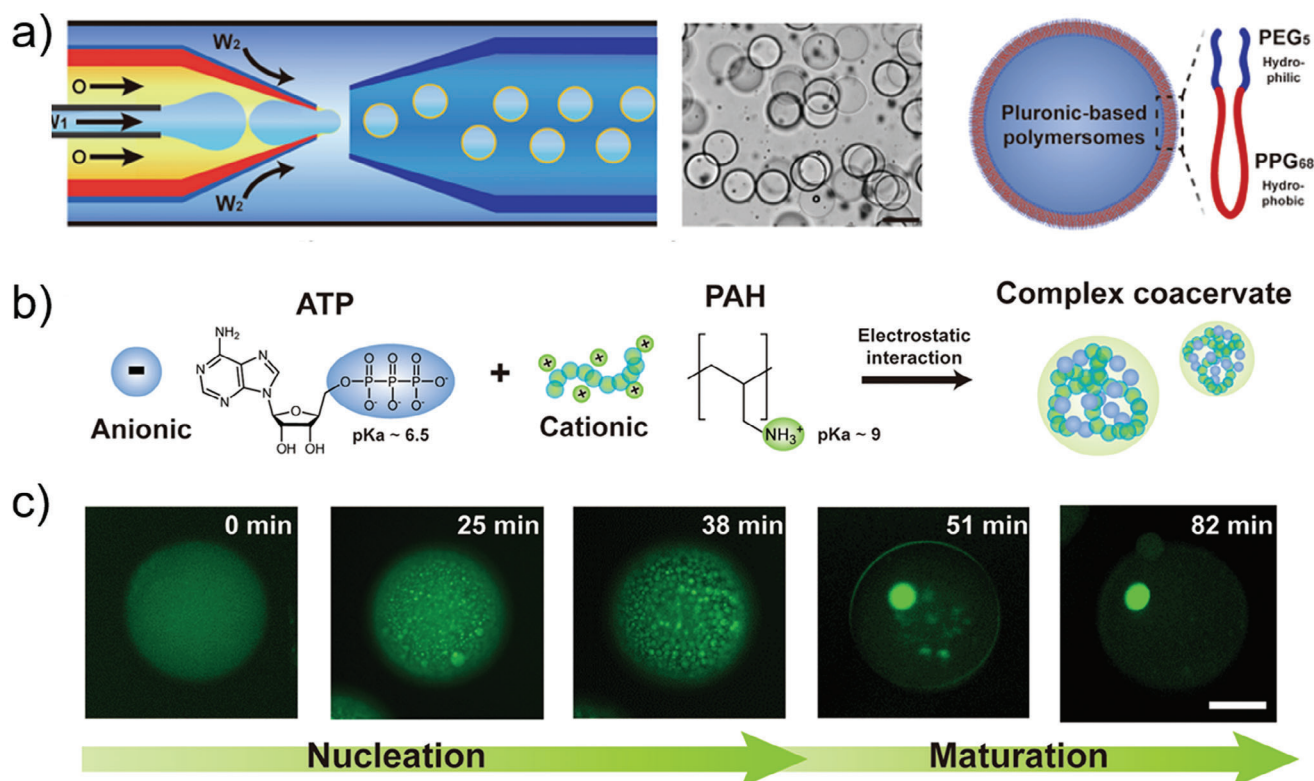
In addition to biomedical applications, polymersomes can also act as components for the construction of artificial cells.[83–85] Peters et al. developed an artificial cell by encapsulating semipermeable small polymersomes within giant polymersomes, resulting in a multi-compartmentalized structure. They employed a three-enzyme cascade reaction model to illustrate the advantages of a multi-compartmentalized system in simulating cell communication processes.[86] Using physical separation by compartmentalization enzymes were protected against the activity of a co-encapsulated protease. In a similar fashion, Mason et al. prepared an artificial cell by loading polymersomes into coacervates (**Figure 8**a).[87] The encapsulation of polymersomes can allow for precise separation of components and therefore enable the study of chemical systems or enzymatic networks in a cell-mimetic environment (Figure 8b).

Seo and colleagues prepared cell-like polymersomes by a microfluidic strategy. Their membrane exhibited size-selective features and was permeable to protons and small molecules (molecular weight cut-off value of 500 Da), as confirmed by the pH-induced formation of coacervates inside of the polymersomes (**Figure 9**a). They utilized the phosphoenol pyruvate-driven enzymatic reaction for the conversion of adenosine diphosphate to

adenosine triphosphate (ATP), which led to electrostatic interactions between ATP and poly(allyl amine hydrochloride) (PAH) to form complex coacervates inside polymersomes (Figure 9b). Additionally, they used this signal-driven enzymatic reaction to facilitate cascade reactions and reconstruct the cytoskeleton within polymersomes through the polymerization of actin monomers into filamentous networks (Figure 9c).[88]

In another example, Meier et al. developed a self-assembled vesicular multicompartment system consisting of a polymeric membrane (a giant unilamellar vesicle, or GUV) made from a mixture of poly(2-methyl-2-oxazoline)$_5$–block–poly(dimethylsiloxane)$_{58}$–block–poly(2-methyl-2-oxazoline)$_5$ (PMOXA$_5$-b-PDMS$_{58}$-b-PMOXA$_5$) and PDMS$_{65}$-b-heparin copolymers that encapsulated artificial organelles. Complex signal transduction in this system was achieved through a lipase reaction involving two different types of artificial organelles. The lipase substrate, 1,2-di-O-lauryl-rac-glycero-3-(glutaric acid 6-methylresorufin ester) (DGGR), was incorporated into a reductively responsive artificial organelle (NPGraft), while the lipase enzyme was encapsulated in a secondary artificial organelle (LipVes). Both types of organelles were then loaded into the GUVs, forming a stimuli-responsive multicompartment system (**Figure 10**a). Under reductive conditions, the DGGR was released from the NP-graft subcompartment, allowing it to interact with the lipase enzyme in LipVes. This reaction produced a fluorescent product upon the addition of the signaling molecule DTT to the GUVs (Figure 10b).[89]

Enzyme-loaded polymersomes, functioning as bio-nanoreactors, have also been utilized in in vivo biomedical applications.[90] Kataoka et al. developed semipermeable,

**ADVANCED
SCIENCE NEWS**

www.advancedsciencenews.com
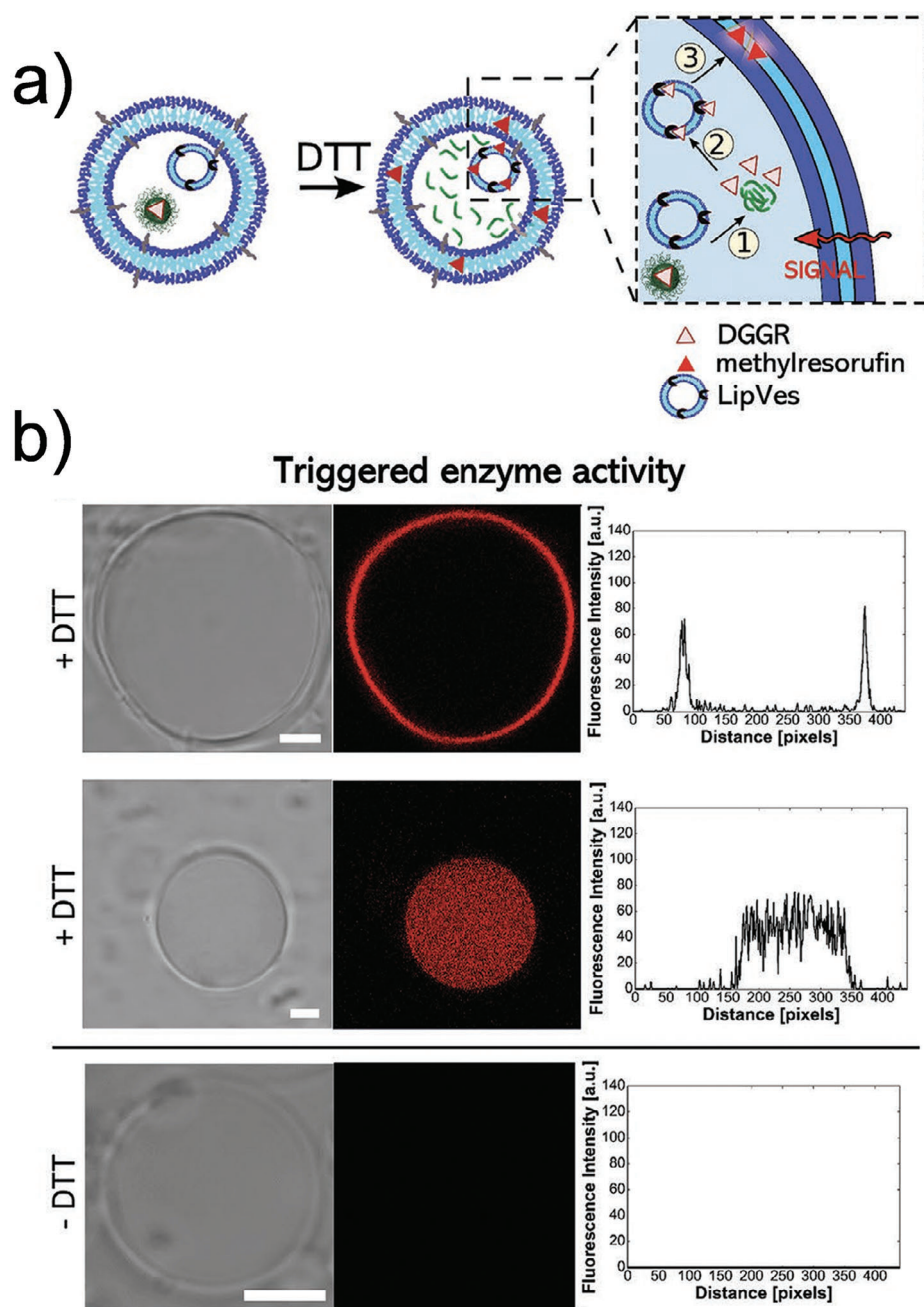
[M] acro-
olecular

Bioscience

www.mbs-journal.de

Figure 9. Polymersomes as artificial organelles to achieve spatiotemporal control of enzymatic reactions. a) Schematic illustration and optical micrograph showing the production of Pluronic-based polymersomes via a glass capillary-based microfluidic device using water-in-oil-in-water double emulsion droplets as templates. Scale bar represents 100 μm. b) Schematics illustrating the complex coacervate formation between adenosine triphosphate and poly(allylamine hydrochloride). c) Series of magnified fluorescence micrographs showing the coacervation process from nucleation to maturation. Scale bar represents 100 μm. Reproduced under terms of the CC-BY-NC license.[88]

enzyme-loaded polyion complex vesicles (PICsomes) using a simple protein-loading method.[91] By combining PEG-based aniomers (PEG-*b*-PAsp), catiomers (homo-P(Asp-AP)), and *β*-galactosidase (*β*-gal), they created *β*-gal-loaded PICsomes (*β*-gal@PICsomes) with a diameter of 100 nm (**Figure 11a**). These *β*-gal@Cy5-PICsomes, along with free *β*-gal, were separately injected intravenously into the tail veins of mice with C26 tumors. Four days later, the model produg HMDER-*β*-gal was administered. The results showed that only the *β*-gal@Cy5-PICsomes selectively accumulated in the tumor tissue, exhibiting significant fluorescence due to the delivery of *β*-gal by the PICsomes and the in situ catalytic conversion of HMDER-*β*-gal into HMDER (Figure 11b). In contrast, free *β*-gal was rapidly cleared from the system, and no detectable HMDER fluorescence was observed after HMDER-*β*-gal injection. *Ex vivo* fluorescence imaging further confirmed that the majority of the generated HMDER fluorescence was concentrated in the tumor tissue (Figure 11c).

5.2. Non-Spherical Polymersomes

In drug delivery applications, it is widely acknowledged that not only the size but also the shape of the carrier significantly influences biodistribution and cellular internalization.[92–94] Conse-

quently, scientists are actively engaged in investigating the formation of polymersomes with non-spherical structures to fulfill the diverse requirements of biomedical applications. One strategy for controlling shape transformation was elucidated by our group. We demonstrated that dialysis could be employed to reshape spherical polymersomes in a range of different topologies.[95] After assembly of polymers in a mixture of water and polar organic solvent, the lumen of the polymersomes typically comprises 50% vol. of organic solvent. Replacing the organic solvent with water by dialysis is an out-of-equilibrium process, as the organic solvent is released faster than water can replenish the lost volume. This depletion forces the polymersome to adopt a different shape, which becomes kinetically trapped as the membrane loses its dynamic character. The spontaneous curvature of the polymer membrane determines whether this shape change process leads to the formation of so-called oblates (discs and bowl-shaped particles, known as stomatocytes), or prolates (tube-like structures).[96–98] The adoption of non-spherical structures provides vesicles with greater versatility and expands their potential applications, such as the development of active, self-propelled nanomotors. These nanomotors, which can move autonomously, significantly enhance the efficiency of drug delivery, especially in overcoming barriers like the blood-brain barrier.[99] In particular, the stomatocyte structure allows for the encapsulation of catalysts within its cavity, enabling the consumption of fuel to

ADVANCED
SCIENCE NEWS

www.advancedsciencenews.com

[M] acro-
olecular
Bioscience

www.mbs-journal.de

Figure 10. Polymersomes as artificial organelles to achieve selective reduction control of enzymatic reactions. a) Schematic representation of the enzymatic reaction of substrate (DGGR)-loaded nanoparticles and enzyme (lipase)-adsorbed polymersomes (LipVes), and their encapsulation as subcompartments into a GUV. b) CLSM imaging of DGGR loaded nanoparticles and LipVes in GUVs in presence (top, middle) and absence (bottom) of DTT. Bright-field images (left), fluorescence images (center), and histograms along the diagonal of the fluorescent images (right). Reproduced under terms of the Creative Commons CC BY.[89] Copyright 2020, Wiley-VCH.

power the nanomotor. For example, in our group we demonstrated that these stomatocytes can function as nanomotors when hydrogen peroxide-consuming catalysts are loaded into their cavities. In the presence of fuel, the incorporation of enzymes enabled the self-propulsion of the stomatocytes.[100] Following this strategy, Tu et al. synthesized PtNP-loaded stomatocyte nanomotors, followed by the conjugation of a temperature-sensitive

poly(N-isopropyl acrylamide) (PNIPAM) polymer brush onto the nanomotor through surface-initiated atom-transfer radical polymerization. This work introduces the first nanoscale chemically driven nanomotor whose motion can be reversibly controlled by a thermal-responsive valve.[101] In addition to entrapping catalytic nanoparticles during the shape transformation process, they can also be encapsulated via an in situ growth method. Pijpers et al.
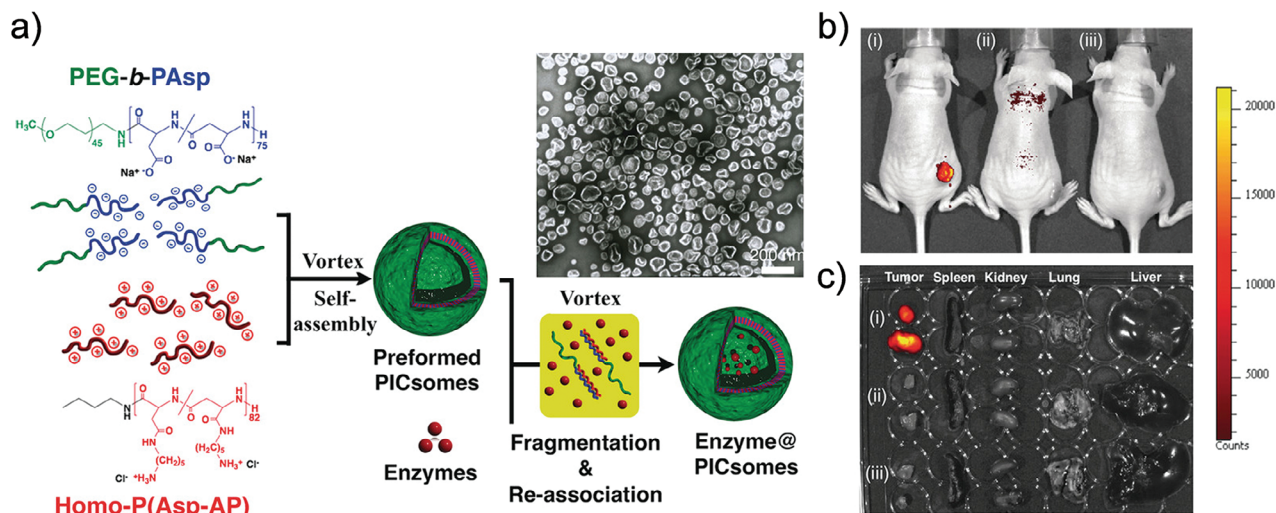
Figure 11. Polymersomes as nanoreactors for biomedical applications. a) Schematic representation of PICsomes and enzyme@PICsomes via preformed PICsomes. Scale bar represents 200 nm. b) In vivo imaging of C26 tumor-bearing mice. The tumor site of the mouse was treated with (I) β-Gal@Cy5-PICsomes, (II) free β-Gal, and (III) HMDER-β-Gal. c) The ex vivo fluorescence imaging of organs. Reproduced with permission.[91] Copyright 2016, Wiley-VCH.

prepared hybrid nanomotors using an in situ one-pot preparation method, employing PDLLA-based stomatocytes as templates for the growth of manganese dioxide (MnO_2) nanoparticles within their cavities (**Figure 12**a). These hybrid nanomotors exhibited high biocompatibility and achieved autonomous motion in the presence of fuel (H_2O_2), enabling effective penetration into 3D tumor cell spheroids (Figure 12b).[102]

Leveraging the shape transformation of polymersomes, Wauters and colleagues systematically investigated the effects of shape and size of antibody-displaying polymersomes on T cell activation.[103] They found that larger polymersomes with a higher antibody density were most effective in enhancing T cell activation, while at low antibody density, elongated polymersomes were more advantageous than their spherical counterparts. Besides stomatocytes and tubes, polymersomes have the capability to transform into other shapes such as peanut and cucurbit-like morphologies.[104,105] For example, Wang et al. prepared peanut-shaped AIE polymersomes for active cargo transportation.[104] These peanut-shaped polymersomes not only generated ROS but also exhibited movement during laser irradiation. This phenomenon arose from the non-spherical structure creating ROS gradients around the particles. Finally, they utilized
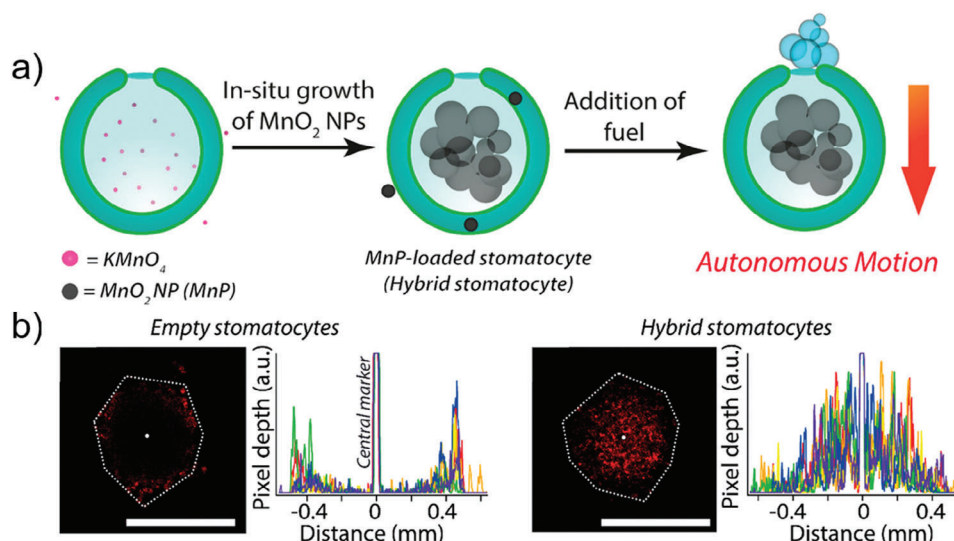
Figure 12. MnO_2-loaded stomatocytes as bubble propulsion nanomotors for effective tumor penetration. a) Schematic demonstrating the compartmentalized synthesis of MnPs within the stomatocytes' lumen and subsequent formation of hybrid nanomotors that can convert fuel into mechanical motion. b) Penetration of empty stomatocytes (left) and hybrid nanomotors (right) into 3D cell spheroids. Scale bars represent 1 mm. Reproduced under terms of the CC-BY-NC-ND license.[102]

**ADVANCED
SCIENCE NEWS**

www.advancedsciencenews.com

Macro-
olecular
Bioscience

www.mbs-journal.de

this multifunctional platform for active cargo transportation and cancer therapy. While research into these non-spherical polymersomes has only recently begun, they present promising opportunities for biomedical applications.

6. Conclusion and Perspective

Polymeric drug carriers serve as versatile platforms for encapsulating various payloads, including drugs, nucleic acids, and proteins. Their usage improves the stability, biocompatibility, and bioavailability of cargo by protecting from the external environment and enabling on-demand release spatially and temporally. While lipid-based nanoparticles currently dominate clinical nanomedicine, significant advancements in polymer chemistry and material science are poised to establish polymeric nanoparticles as the next-generation drug delivery systems in this domain. This shift is attributed to the chemical diversity and straightforward synthesis of polymers compared to lipids. Tailor-made polymers and tunable self-assembly conditions endow the assemblies with useful features that enable their application in drug delivery, therapy, imaging, artificial cell communication, and biocatalysis. In this review, we have provided an overview of common polymeric assemblies, including micelles, spherical and non-spherical vesicles, covering aspects such as design, synthesis, characterization, and their applications. We mainly illustrated these concepts with some leading research examples and results from our group.

Despite significant progress in polymeric cargo carriers, certain aspects still require further development. For example, there is a need for a clearer understanding of the self-assembly mechanism and precise control over the formation of different nanostructures. Achieving efficient and scalable production of polymeric-carrier-based therapeutics will be feasible when the self-assembly process can be conducted on a large scale. Additionally, the design of polymeric drug delivery systems should focus on achieving precisely controllable cargo release. Maintaining drug concentrations within the therapeutic window, ideally between the minimum effective concentration and minimum toxic concentration, is crucial for optimizing therapy.[106] Drug carriers with controllable release capacity offer the potential to achieve this goal. Various functionalities can be incorporated into synthetic polymers through different synthetic strategies to meet these requirements. For instance, smart polymeric assemblies can respond to external stimuli such as light, temperature, pH, or redox changes, altering their shape, size, and properties to achieve controlled cargo release. Furthermore, minimizing drug leakage can be achieved by covalently attaching drug molecules onto polymer chains, thereby reducing the side effects of nanomedicine. Additionally, surface modification techniques can facilitate the incorporation of targeting groups into nanoparticles, enabling precise therapy and imaging. In summary, we anticipate that further exploration of polymer chemistry and nanotechnology tools will provide numerous opportunities for the clinical translation of polymeric drug delivery systems.

## Conflict of Interest

The authors declare no conflict of interest.

[1] I. Negut, B. Bita, *Pharmaceutics* **2023**, *15*, 976.
[2] M. G. Gouveia, J. P. Wesseler, J. Ramaekers, C. Weder, P. B. V. Scholten, N. Bruns, *Chem. Soc. Rev.* **2023**, *52*, 728.
[3] E. Rideau, R. Dimova, P. Schwille, F. R. Wurm, K. Landfester, *Chem. Soc. Rev.* **2018**, *47*, 8572.
[4] S. Kansız, Y. M. Elçin, *Adv. Colloid Interface Sci.* **2023**, 102930.
[5] C. H. Lo, J. Zeng, *Bioeng. Transl. Med.* **2023**, *8*, e10350.
[6] K. Kuperkar, D. Patel, L. I. Atanase, P. Bahadur, *Polymers* **2022**, *14*, 4702.
[7] C. K. Wong, M. H. Stenzel, P. Thordarson, *Chem. Soc. Rev.* **2019**, *48*, 4019.
[8] C. K. Wong, A. D. Martin, M. Floetenmeyer, R. G. Parton, M. H. Stenzel, P. Thordarson, *Chem. Sci.* **2019**, *10*, 2725.
[9] C. K. Wong, R. Y. Lai, M. H. Stenzel, *Nat. Commun.* **2023**, *14*, 6237.
[10] A. Martin, P. Lalanne, A. Weber-Vax, A. Mutschler, S. Lecommandoux, *Int. J. Pharm.* **2023**, *642*, 123157.
[11] D. Patel, K. Kuperkar, S. Yusa, P. Bahadur, *Drugs Drug Candidates* **2023**, *2*, 898.
[12] P. Alexandridis, B. Lindman, Elsevier, **2000**.
[13] C. Hua, L. Qiu, *Int. J. Nanomed.* **2024**, *2024*, 2317.
[14] Y. Zheng, Y. Oz, Y. Gu, N. Ahamad, K. Shariati, J. Chevalier, D. Kapur, N. Annabi, *Nano Today* **2024**, *55*, 102147.
[15] S. Pande, *Artif. Cells Nanomed. Biotechnol.* **2023**, *51*, 428.
[16] W. Shen, W. Liu, H. Yang, P. Zhang, C. Xiao, X. Chen, *Biomaterials* **2018**, *178*, 706.
[17] X. D. Xu, L. Zhao, Q. Qu, J. G. Wang, H. Shi, Y. Zhao, *ACS Appl. Mater. Interfaces* **2015**, *7*, 17371.
[18] S. Cao, Y. Xia, J. Shao, B. Guo, Y. Dong, I. A. B. Pijpers, Z. Zhong, F. Meng, L. K. E. A. Abdelmohsen, D. S. Williams, J. C. M. van Hest, *Angew. Chem., Int. Ed.* **2021**, *60*, 17629.
[19] H. Moulahoum, F. Ghorbanizamani, F. Zihnioglu, S. Timur, *Bioconjug. Chem.* **2021**, *32*, 1491.
[20] X. Li, Y. Wang, Q. Yan, *Angew. Chem., Int. Ed.* **2023**, *62*, 202305290.
[21] R. A. J. F. Oerlemans, J. Shao, S. G. A. M. Huisman, Y. Li, L. K. E. A. Abdelmohsen, J. C. M. van Hest, *Macromol. Rapid Commun.* **2023**, *44*, 2200904.
[22] J. Shao, S. Cao, H. Che, M. T. D. Martino, H. Wu, L. K. E. A. Abdelmohsen, J. C. M. van Hest, *J. Am. Chem. Soc.* **2022**, *144*, 11246.
[23] J. Han, Y. Liu, D. Peng, J. Liu, D. Wu, *Bioconjug. Chem.* **2023**, *34*, 2155.
[24] F. Araste, A. Aliabadi, K. Abnous, S. M. Taghdisi, M. Ramezani, M. Alibolandi, *J. Controlled Release* **2021**, *330*, 502.
[25] J. Zhang, J. Jiang, S. Lin, E. J. Cornel, C. Li, J. Du, *Chinese J. Chem.* **2022**, *40*, 1842.
[26] F. Perin, A. Motta, D. Maniglio, *Mater. Sci. Eng. C* **2021**, *123*, 111952.

[27] P. Gurnani, S. Perrier, *Prog. Polym. Sci.* **2020**, *102*, 101209.

[28] K. Matyjaszewski, *Adv. Mater.* **2018**, *30*, 1706441.

[29] M. Kato, M. Kamigaito, M. Sawamoto, T. Higashimura, *Macromolecules* **1995**, *28*, 1721.

[30] K. Matyjaszewski, J. Xia, *Chem. Rev.* **2001**, *101*, 2921.

[31] Q. Wang, X. Feng, X. Liu, *Cellulose* **2023**, *30*, 8495.

[32] J. Chiefari, Y. K. Chong, F. Ercole, J. Krstina, J. Jeffery, T. P. T. Le, R. T. A. Mayadunne, G. F. Meijs, *Macromolecules* **1998**, *31*, 5559.

[33] K. Matyjaszewski, J. Xia, *Handbook of Radical Polymerization*, John Wiley & Sons, Hoboken, **2002**.

[34] U. C. Palmiero, M. Sponchioni, N. Manfredini, M. Maraldi, D. Moscatelli, *Polym. Chem.* **2018**, *9*, 4084.

[35] V. C. F. Mosqueira, P. Legrand, J. L. Morgat, M. Vert, E. Mysiakine, R. Gref, J. P. Devissaguet, G. Barratt, *Pharm. Res.* **2001**, *18*, 1411.

[36] Y. Zhang, X. Liu, P. He, B. Tang, C. Xiao, X. Chen, *Biomacromolecules* **2023**, *24*, 4316.

[37] P. L. W. Welzen, S. W. M. Ciriano, S. Cao, A. F. Mason, I. A. B. Welzen-Pijpers, J. C. M. van Hest, *J. Appl. Polym. Sci.* **2021**, *59*, 1241.

[38] M. Elsabahy, K. L. Wooley, *Chem. Soc. Rev.* **2012**, *41*, 2545.

[39] B. J. Toebes, D. A. Wilson, *Soft Matter.* **2021**, *17*, 1724.

[40] Z. Lin, S. Liu, W. Mao, H. Tian, N. Wang, N. Zhang, F. Tian, L. Han, X. Feng, Y. Mai, *Angew. Chem., Int. Ed.* **2017**, *129*, 7241.

[41] C. Li, Q. Li, Y. V. Kaneti, D. Hou, Y. Yamauchi, Y. Mai, *Chem. Soc. Rev.* **2020**, *49*, 4681.

[42] M. Müller, *Prog. Polym. Sci.* **2020**, *101*, 101198.

[43] C. Guo, H. Yuan, Y. Zhang, T. Yin, H. He, J. Gou, X. Tang, *J. Controlled Release* **2021**, *338*, 422.

[44] Y. Mai, A. Eisenberg, *Chem. Soc. Rev.* **2012**, *41*, 5969.

[45] A. Sorrenti, J. Leira-Iglesias, A. J. Markvoort, T. F. A. de Greef, T. M. Hermans, *Chem. Soc. Rev.* **2017**, *46*, 5476.

[46] M. Fonseca, I. Jarak, F. Victor, C. Domingues, F. Veiga, A. Figueiras, *Materials* **2024**, *17*, 319.

[47] K. F. Castillo-Romero, A. Santacruz, J. González-Valdez, *Electrophoresis* **2023**, *44*, 107.

[48] S. Pearce, J. Perez-Mercader, *Polym. Chem.* **2021**, *12*, 29.

[49] B. Karagoz, L. Esser, H. T. Duong, J. S. Basuki, C. Boyer, T. P. Davis, *Polym. Chem.* **2014**, *5*, 350.

[50] Y. Dou, B. Wang, M. Jin, Y. Yu, G. Zhou, L. Shui, *J. Micromech. Microeng.* **2017**, *27*, 113002.

[51] J. K. Salem, I. M. El-Nahhal, S. F. Salama, *Chem. Phys. Lett.* **2019**, *730*, 445.

[52] G. Riess, *Prog. Polym. Sci.* **2003**, *28*, 1107.

[53] X. Wang, M. Zhang, Y. Li, H. Cong, B. Yu, Y. Shen, *Small* **2023**, *19*, 2304006.

[54] N. Hueppe, F. R. Wurm, K. Landfester, *Macromol. Rapid Commun.* **2023**, *44*, 2200611.

[55] A. Figueiras, C. Domingues, J. I., A. I. Santos, A. Parra, A. Pais, C. Alvarez-Lorenzo, A. Concheiro, A. Kabanov, H. Cabral, F. Veiga, *Pharmaceutics* **2022**, *14*, 1700.

[56] X. Yang, Z. Li, N. Wang, L. Li, L. Song, T. He, L. Sun, Z. Wang, Q. Wu, N. Luo, C. Yi, C. Gong, *Sci. Rep.* **2015**, *5*, 10322.

[57] D. Zhang, Z. Zou, W. Ren, H. Qian, Q. Cheng, L. Ji, B. Liu, Q. Liu, *Pharm. Dev. Technol.* **2018**, *23*, 33.

[58] Y. Jiaying, S. Bo, W. Xiaolu, Z. Yanyan, W. Hongjie, S. Nan, G. Bo, W. Linna, Z. Yan, G. Wenya, L. Keke, J. Shan, L. Chuan, Z. Yu, Z. Qinghe, Z. Haiyu, *Drug Delivery* **2023**, *30*, 2177362.

[59] S. Guan, Q. Zhang, J. Bao, T. Duan, R. Hu, T. Czech, J. Tang, *Eur. J. Pharm. Biopharm.* **2020**, *147*, 87.

[60] J. Sun, H. Yao, X. Ren, L. Cui, L. Liu, G. Wang, Z. Tang, *Nano Lett.* **2024**, *24*, 2921.

[61] Q. Zhang, P. Yu, Y. Fan, C. Sun, H. He, X. Liu, L. Lu, M. Zhao, H. Zhang, Z. F., *Angew. Chem., Int. Ed.* **2021**, *133*, 4013.

[62] B. Liu, J. Jiao, W. Xu, M. Zhang, P. Cui, Z. Guo, Y. Deng, H. Chen, W. Sun, *Adv. Mater.* **2021**, *33*, 2100795.

[63] J. Ren, Y. Cao, L. Li, X. Wang, H. Lu, J. Yang, S. Wang, *J. Controlled Release* **2021**, *338*, 537.

[64] S. Cai, K. Vijayan, D. Cheng, E. M. Lima, D. E. Discher, *Pharm. Res.* **2007**, *24*, 2099.

[65] J. K. Elter, S. Quader, J. Eichhorn, M. Gottschaldt, K. Kataoka, F. H. Schacher, *Biomacromolecules* **2021**, *22*, 1458.

[66] Y. Gao, J. Zhao, X. Zhang, X. Wei, X. Xiong, X. Guo, Z. S., *J. Mater. Chem. B* **2017**, *5*, 4943.

[67] L. Zhang, A. Eisenberg, *Science* **1995**, *268*, 1728.

[68] J. C. M. Van Hest, D. A. P. Delnoye, M. Baars, M. H. P. Van Genderen, E. W. Meijer, *Science* **1995**, *268*, 1592.

[69] D. E. Discher, F. Ahmed, *Annu. Rev. Biomed. Eng.* **2006**, *8*, 323.

[70] B. M. Discher, Y. Y. Won, D. S. Ege, J. C. M. Lee, F. S. Bates, D. E. Discher, D. A. Hammer, *Science* **1999**, *284*, 1143.

[71] H. Lomas, I. Canton, S. MacNeil, J. Du, S. P. Armes, A. J. Ryan, A. L. Lewis, G. Battaglia, *Adv. Mater.* **2007**, *19*, 4238.

[72] T. O. Pangburn, M. A. Petersen, B. Waybrant, M. M. Adil, E. Kokkoli, *J. Biomech. Eng.* **2009**, *131*, 074005.

[73] F. Meng, Z. Zhong, *J. Phys. Chem. Lett.* **2011**, *2*, 1533.

[74] R. P. Brinkhuis, F. P. J. T. Rutjes, J. C. M. van Hest, *Polym. Chem.* **2011**, *2*, 1449.

[75] M. Beygi, F. Oroojalian, S. S. Hosseini, A. Mokhtarzadeh, P. Kesharwani, A. Sahebkar, *Prog. Mater. Sci.* **2023**, *140*, 101209.

[76] A. C. Wauters, J. F. Scheerstra, M. M. van Leent, A. J. P. Teunissen, B. Priem, T. J. Beldman, N. Rother, R. Duivenvoorden, G. Prévot, J. Munitz, Y. C. Toner, J. Deckers, Y. van Elsas, P. Mora-Raimundo, G. Chen, S. A. Nauta, A. V. D. Verschuur, A. W. Griffioen, D. P. Schrijver, T. Anbergen, Y. Li, H. Wu, A. F. Mason, M. H. M. E. van Stevendaal, E. Kluza, R. A. J. Post, L. A. B. Joosten, M. G. Netea, C. Calcagno, Z. A. Fayad, et al., *Nat. Nanotechnol.* **2024**, *19*, 1735.

[77] D. Zhu, S. Wu, C. Hu, Z. Chen, H. Wang, F. Fan, Y. Qin, C. Wang, H. Sun, X. Leng, D. Kong, L. Zhang, *Acta Biomater.* **2017**, *58*, 399.

[78] J. Shao, S. Cao, D. S. Williams, L. K. E. A. Abdelmohsen, J. C. M. van Hest, *Angew. Chem., Int. Ed.* **2020**, *59*, 16918.

[79] L. Yan, E. Higbee, A. Tsourkas, Z. Cheng, *J. Mater. Chem. B* **2015**, *3*, 9277.

[80] S. Cao, J. Shao, H. Wu, S. Song, M. T. D. Martino, I. A. B. Pijpers, H. Friedrich, L. K. E. A. Abdelmohsen, D. S. Williams, J. C. M. van Hest, *Nat. Commun.* **2021**, *12*, 2077.

[81] Y. Luo, H. Wu, X. Zhou, J. Wang, S. Er, Y. Li, P. L. W. Welzen, R. A. J. F. Oerlemans, L. K. E. A. Abdelmohsen, J. Shao, J. C. M. van Hest, *J. Am. Chem. Soc.* **2023**, *145*, 20073.

[82] Z. P. Wang, M. C. M. van Oers, F. P. J. T. Rutjes, J. C. M. van Hest, *Angew. Chem., Int. Ed.* **2012**, *51*, 10746.

[83] V. Maffeis, L. Heuberger, A. Nikoletić, C. Schoenenberger, C. G. Palivan, *Adv. Sci.* **2024**, *11*, 2305837.

[84] B. C. Buddingh', J. C. M. van Hest, *Acc. Chem. Res.* **2017**, *50*, 769.

[85] K. Ngocho, X. Yang, Z. Wang, C. Hu, X. Yang, H. Shi, K. Wang, J. Liu, *Small* **2024**, 2400086.

[86] R. J. R. W. Peters, M. Marguet, S. Marais, M. W. Fraaije, J. C. M. van Hest, S. Lecommandoux, *Angew. Chem., Int. Ed.* **2014**, *126*, 150.

[87] A. F. Mason, N. A. Yewdall, P. L. W. Welzen, J. Shao, M. van Stevendaal, J. C. M. van Hest, D. S. Williams, L. K. E. A. Abdelmohsen, *ACS Cent. Sci.* **2019**, *5*, 1360.

[88] H. Seo, H. Lee, *Nat. Commun.* **2022**, *13*, 5179.

[89] A. Belluati, S. Thamboo, A. Najer, V. Maffeis, C. Planta, I. Craciun, C. G. Palivan, W. Meier, *Adv. Funct. Mater.* **2020**, *30*, 2002949.

[90] G.-G. M., M. J. York-Duran, L. Hosta-Rigau, *Adv. Healthcare Mater.* **2018**, *7*, 1700917.

[91] Y. Anraku, A. Kishimura, M. Kamiya, S. Tanaka, T. Nomoto, K. Toh, Y. Matsumoto, S. Fukushima, D. Sueyoshi, M. R. Kano, Y. Urano, N. Nishiyama, K. Kataoka, *Angew. Chem., Int. Ed.* **2016**, *55*, 560.

[92] V. P. Chauhan, Z. Popović, O. Chen, J. Cui, D. Fukumura, M. G. Bawendi, R. K. Jain, *Angew. Chem., Int. Ed.* **2011**, *50*, 11417.

2400540 (14 of 16)

[93] J. A. Champion, Y. K. Katare, S. Mitragotri, *J. Controlled Release* **2007**, *121*, 3.

[94] P. Decuzzi, R. Pasqualini, W. Arap, M. Ferrari, *Pharm. Res.* **2009**, *26*, 235.

[95] K. T. Kim, J. Zhu, S. A. Meeuwissen, J. J. L. M. Cornelissen, D. J. Pochan, R. J. M. Nolte, J. C. M. van Hest, *J. Am. Chem. Soc.* **2010**, *132*, 12522.

[96] H. Che, J. Zhu, S. Song, A. F. Mason, S. Cao, I. A. B. Pijpers, L. K. E. A. Abdelmohsen, J. C. M. van Hest, *Angew. Chem., Int. Ed.* **2019**, *58*, 13113.

[97] J. Shao, S. Cao, H. Wu, L. K. E. A. Abdelmohsen, J. C. M. van Hest, *Pharmaceutics* **2021**, *13*, 1833.

[98] F. Peng, Y. Tu, J. C. M. Van Hest, D. A. Wilson, *Angew. Chem., Int. Ed.* **2015**, *54*, 11662.

[99] W. Zhang, Z. Zhang, S. Fu, Q. Ma, Y. Liu, N. Zhang, *ChemPhysMater* **2023**, *2*, 114.

[100] D. A. Wilson, R. J. M. Nolte, J. C. M. Van Hest, *Nat. Chem.* **2012**, *4*, 268.

[101] Y. Tu, F. Peng, X. Sui, Y. Men, P. B. White, J. C. M. van Hest, D. A. Wilson, *Nat. Chem.* **2017**, *9*, 480.

[102] I. A. B. Pijpers, S. Cao, A. Llopis-Lorente, J. Zhu, S. Song, R. R. M. Joosten, F. Meng, H. Friedrich, D. S. Williams, S. Sánchez, J. C. M. Van Hest, L. K. E. A. Abdelmohsen, *Nano Lett.* **2020**, *20*, 4472.

[103] A. C. Wauters, J. F. Scheerstra, I. G. Vermeijlen, R. Hammink, M. Schluck, L. Woythe, H. Wu, L. Albertazzi, C. G. Figdor, J. Tel, L. K. E. A. Abdelmohsen, J. C. M. van Hest, *ACS Nano* **2022**, *16*, 15072.

[104] J. Wang, Y. Luo, H. Wu, S. Cao, L. K. E. A. Abdelmohsen, J. Shao, J. C. M. van Hest, *Pharmaceutics* **2023**, *15*, 1986.

[105] S. Cao, H. Wu, I. A. B. Pijpers, J. Shao, L. K. E. A. Abdelmohsen, D. S. Williams, J. C. M. Van Hest, *ACS Nano* **2021**, *15*, 18270.

[106] C. Moore, F. Chen, J. Wang, J. V. Jokerst, *Adv. Drug Delivery Rev.* **2019**, *144*, 78.
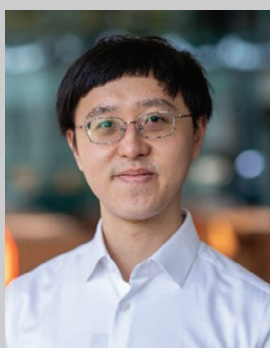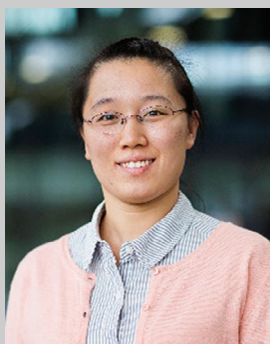
Yingtong Luo received his B.Sc. degree in chemistry from China West Normal University. Afterward, he started his M.Sc project at South China Normal University, focusing on the "Design, Synthesis, and Photoacoustic Imaging Applications of Near-infrared Conjugated Polymers" supervised by Prof. Shengjian Liu. Currently, he is a Ph.D. candidate at Eindhoven University of Technology, engineering photothermal responsive polymeric nanoparticles for bio-applications under the supervision of Prof. Jan C. M. van Hest & Dr. Jingxin Shao.
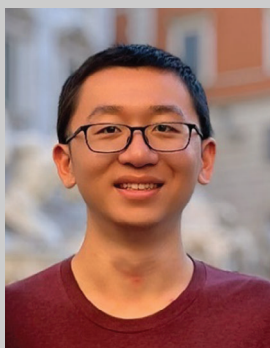
Yudong Li received his B.Eng. degree in biomedical engineering from Zhejiang University. Afterward, he worked on point-of-care testing for infectious disease detection at Brigham and Women's Hospital, Harvard Medical School. Then he started his MRes project at Imperial College London and worked on photoresponsive polymersomes supervised by Prof. Molly M. Stevens. Currently, he is a Ph.D. candidate at Eindhoven University of Technology (TU/e), engineering functional polymeric assemblies for nanomedicine under the supervision of Prof. Jan van Hest and Dr. Loai Abdelmohsen.

Loai Abdelmohsen is an assistant professor in the Department of Chemical Engineering and Chemistry at TU/e and manager of Interactive Polymer Materials (IPM) research center. He obtained his Ph.D. in the Bio-Organic Chemistry group, at Radboud University Nijmegen in 2017. Loai's research is focused on the utilization of copolymers for supramolecular assembly and the subsequent integration of functional properties.

2400540 (15 of 16)

ADVANCED
SCIENCE NEWS

www.advancedsciencenews.com

Macromolecular
Bioscience

www.mbs-journal.de

Jingxin Shao obtained her Ph.D. in Chemical Engineering and Technology from the Harbin Institute of Technology under the supervision of Prof. Qiang He. Following her Ph.D., she joined the Bio-Organic Chemistry research group led by Prof. Jan C. M. van Hest at Eindhoven University of Technology in the Netherlands as a Postdoctoral Researcher. Her research interests focus on self-assembled supramolecular micro- and nanoarchitectures, life-like artificial cells, bio-inspired micro- and nanomachines, and their applications in biomedicine.

Jan van Hest obtained his Ph.D. from Eindhoven University of Technology in 1996 with prof E.W. Meijer. He worked as a postdoc with prof D. A. Tirrell on protein engineering. In 2000 he was appointed full professor at Radboud University Nijmegen. As of September 2016, he holds the chair of Bio-organic Chemistry at Eindhoven University of Technology. He is the scientific director of the Institute for Complex Molecular Systems (ICMS). The group's focus is, by using a combination of synthetic techniques, to develop well-defined compartments for nanomedicine and artificial cell research, with application potential in, e.g., cancer treatment and immunology.